Characterization of Hydrogen Bonding in the Complex of Adenosine Deaminase with a Transition State Analogue: A Raman Spectroscopic Study†

Hua Deng,‡ Linda C. Kurz,§ Frederick B. Rudolph,‖ and Robert Callender*,⊥

Physics Department, City College of the City University of New York, New York, New York 10031, Department of Biochemistry and Molecular Biophysics, Washington University School of Medicine, St. Louis, Missouri 63110, Department of Biochemistry and Cell Biology and The Institute of Biosciences and Bioengineering, Rice University, Houston, Texas 77005, and Department of Biochemistry, Albert Einstein College of Medicine, Bronx, New York 10461

Received November 13, 1997; Revised Manuscript Received January 27, 1998

ABSTRACT: The Raman spectra of purine ribonucleoside as well as a stable model compound (1-methoxyl-1,6-dihydropurine ribonucleoside), free in solution and bound into its complex with adenosine deaminase (ADA), have been studied by Raman difference spectroscopy. Using purine riboside analogues labeled with ^{15}N1 or ^{13}C6 and the theoretical frequency normal-mode analyses of these molecules using ab initio quantum mechanic methods, we have positively identified many of the Raman bands in the enzyme-bound inhibitor. The spectrum of the enzyme-bound inhibitor is consistent with the enzyme-catalyzed hydration of the purine base to yield 1-hydroxyl-1,6-dihydropurine ribonucleoside, as suggested earlier by X-ray crystallographic studies. In addition, the Raman data and subsequent vibrational analyses show that the binding-induced Raman spectral changes of the inhibitor can be modeled by the formation of a strong hydrogen bond to its N1−H bond. This hydrogen bond, apparently between the N1−H of the inhibitor and the Oδ1 of Glu217 in ADA, causes a substantial N1−H bending frequency increase of about 50−100 cm^{-1} compared to its solution value, and this results in an estimated enthalpy of the hydrogen bond of 4−10 kcal/mol. The relationship of transition state stabilization in the catalytic strategy of this efficient enzyme to such a bonding pattern is discussed.

Adenosine deaminase (ADA)[1] catalyzes the hydrolysis of adenosine or deoxyadenosine to their respective inosine product and ammonia. Purine ribonucleoside is a competitive inhibitor of adenosine deaminase, with an apparent inhibition constant of 2.8×10^{-6} M (*1*). Carbon-13 NMR measurements have suggested that in its complex with adenosine deaminase, purine ribonucleoside (Scheme 1) is hydrated at the N1 and C6 positions to yield 6-hydroxyl-1,6-dihydropurine ribonucleoside (DHPR) (*2*). Subsequent X-ray crystallographic studies have confirmed this suggestion (*3*). The structure of the ADA/6-hydroxyl-1,6-dihydroxylpurine ribonucleoside (ADA−DHPR) complex shows that the bound inhibitor is tightly held in place by nine hydrogen bonds and by a coordination of the 6-hydroxyl group to a zinc ion (*3*). Since the deamination reaction pathway is expected to have a transition state (or intermediate) in which N1 is protonated and C6 becomes tetrahedral, the ADA/DHPR complex is believed to be a very good transition state (or intermediate) analogue (*3*). Correcting the apparent inhibition constant for the unfavorable hydration equilibrium (*4*), the true affinity of the hydrated purine riboside, $K_i = 1.6 \times 10^{-13}$ M, approaches that expected for the transition state of the deamination reaction ($K_{ts} = 3 \times 10^{-17}$ M).

Scheme 1

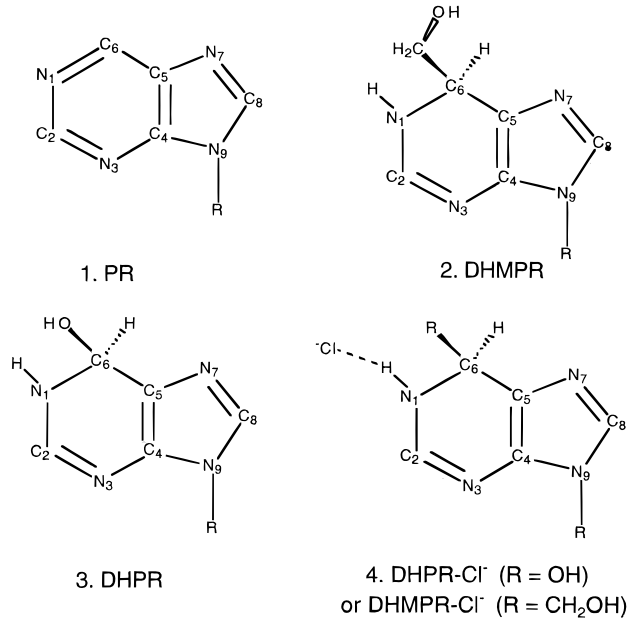

Since the purine ring is hydrated when PR binds to ADA, the aromaticity of the pyridinium ring of the purine heterocycle is expected to be disrupted. We report here Raman

† This work was supported by grants GM35183 (R.C.), GM33851 (L.C.K.), and GM42436 (F.B.R.) from the National Institutes of Health, Institute of General Medicine, and by Grant C-1372 (Rice University) from the Robert A Welch Foundation.

‡ City College of the City University of New York.
§ Washington University School of Medicine.
‖ Rice University.
⊥ Albert Einstein College of Medicine.

[1] Abbreviations: ADA, adenosine deaminase; DHPR, 1-hydroxyl-1,6-dihydropurine ribonucleoside; DHMPR, 1-methoxyl-1,6-dihydropurine ribonucleoside; PR, purine ribonucleoside; OMA, multichannel analyzer.

S0006-2960(97)02790-6 CCC: $15.00
Published on Web 03/19/1998

difference spectroscopic studies (for a review, see *5*) of the ADA/DHPR complex and compare them with data from similar studies of model compounds and the predictions of theoretical calculations using ab initio methods. Large changes in the PR Raman spectrum are observed upon binding, and the results confirm that the hydration of the inhibitor occurs upon binding as suggested in the previous NMR and crystallographic studies. In addition, the results suggest that the interaction between ADA and bound DHPR involves a strong hydrogen bond to the N1−H bond of DHPR, which is at least partly responsible for transition state stabilization in the catalytic strategy of this efficient enzyme.

MATERIALS AND METHODS

Materials. Mouse adenosine deaminase was overexpressed in *E. coli* and harvested and purified according to the procedure described previously (*6*). 1,6-Dihydro-6-(hydroxymethyl)purine riboside (DHMPR) was prepared and fractionated into diastereomers according to published methods, and the *S* isomer, which has a dissociation constant of 0.29×10^{-6} M with ADA, was used in our Raman experiments (*7*). [^{13}C6]Purine riboside was synthesized as previously described (*2*). [^{15}N1]Purine riboside was prepared from [^{15}N1]hypoxanthine following the same procedures for preparing the nucleoside from the base as were used for the ^{13}C6 compound. [^{15}N1]Hypoxanthine was prepared using $^{15}NH_4OH$ (28−30% aqueous solution, Isotec Inc.) based on the published methods (*8, 9*). The ADA sample in 50% glycerol was first dialyzed in 20 mM tris, 10 μM $ZnCl_2$, and 0.2 mM DTT buffer at pH7.5. After dialysis, the sample was concentrated by a Centricon30 centrifuge concentrator to 4 mM. The deuterated sample was prepared by washing the concentrated sample in Centricon30 twice with the above buffer prepared in D_2O. The inhibitor was then added to the enzyme sample so that the final concentration ratio of ADA/inhibitor was about 4 mM/3.5 mM. The following extinction coefficients were used to calculate the sample concentrations: for ADA, $\epsilon_{280} = 45\,000$ M^{-1} cm^{-1}; for DHPR, $\epsilon_{263} = 7350$ M^{-1} cm^{-1}; for DHMPR, $\epsilon_{297} = 4590$ M^{-1} cm^{-1}.

Spectroscopy. The Raman spectra were measured using an optical multichannel analyzer (OMA) system. The OMA system uses a Triplemate spectrometer (Spex Industries, Metuchen, NJ) with a Model DIDA-1000 reticon detector connected to an ST-100 detector (Princeton Instruments, Trenton, NJ). Details of the system can be found elsewhere (*10*). The 514.5 nm line from an argon ion laser (Model 165, Spectra Physics, Mountain View, CA) was used to irradiate the sample (∼100 mW). Separate spectra for enzyme and enzyme·inhibitor complexes in solution, approximate concentration of 4 mM, were measured using a special split cell (the volume of each side being about 30 μL) and a sample holder with a linear translator as previously described (*5*). The spectrum in one side of the split cuvette is taken, the split cell is translated, and the spectrum in the other side is taken. This sequence is repeated until sufficient signal-to-noise is obtained. A difference spectrum is generated by numerically subtracting the sum of the spectra obtained from each side. In general, the two summed spectra do not subtract to zero, as judged by the subtraction of well-known protein marker bands (for example, the amide-I, amide-III, and the 1450 cm^{-1} bands, the latter band being especially useful since it is generally not affected by protein conformational changes). These protein marker bands are determined from their bandwidths (generally much broader than those from spectra of bound substrates) and their characteristic positions. Hence, one summed spectrum is scaled by a small numerical factor, generally between 1.05 and 0.95, which is adjusted until the protein bands are nulled. As an example, the summed spectra and the difference spectra generated by numerical factors somewhat larger to somewhat smaller than that used to generate the difference spectrum in Figure 1c below are shown in the Appendix. Also shown are the primary data and a control measurement whereby the protein binary complex sample is used to generate both the 'sample' as well as the 'reference' spectra. Resolution of the spectrometer is 8 cm^{-1} for the present results. The same control procedures were performed on all the difference spectra with results herein. A spectral calibration is done for each measurement using the known Raman lines of toluene, and absolute band positions are accurate to within ±2 cm^{-1}. None of the spectra presented here have been smoothed.

Computational Methods. The ab initio Hatree−Fock method (using 3-21 g or 6−31 g** basis set), as implemented in Gaussian 94 (*11*), was used to optimize the geometry of the model compounds of PR, DHPR, DHMPR, and DHPR or DHMPR complexed with Cl^- ion at a fixed position (see Scheme 1). The vibrational normal modes were then calculated on these geometrically optimized model compounds. The ribose group (R in Scheme 1) is replaced by a methoxyl group in these calculations to save computer time. Our test runs on a full purine ribose suggest that the ribose ring has only marginal effects on the frequencies of the purine ring modes and especially small effects on the vibrational modes related to the pyridinium ring motions.

RESULTS

The Raman Spectra of Purine Ribonucleoside. The Raman spectra of PR in H_2O and D_2O are reported in Figure 1a,b, respectively. The band at 868 cm^{-1} in Figure 1a shifts down to 849 cm^{-1} when PR is suspended in D_2O (Figure 1b). Since there are no exchangeable hydrogens on the purine ring under our experimental conditions, this band is assigned to the vibrational mode of the ribose moiety. The weak band at 1380 cm^{-1} in Figure 1b is apparently related to the vibrations of the ribose O−D groups. In previous Raman spectroscopic studies, we have shown that the intensities of the vibrational bands from the ribose moiety are generally weaker than those from the purine base (e.g., *12*). Thus, the intense bands in Figure 1a at 797, 1104, 1305, 1358, and 1503 cm^{-1} can be assigned to the vibrational modes from the heterocyclic purine ring of PR.

Figure 1c,d shows the difference Raman spectra between the ADA/PR complex and ADA, prepared in H_2O and D_2O, respectively. These difference spectra contain Raman bands from the bound inhibitor as well as from that of the enzyme (positive or negative) since the protein structure is perturbed upon binding of the inhibitor. Frequency differences in some of the vibrational modes of the protein in the ADA/PR complex and in ADA are expected. Our previous Raman difference experiments on similar enzyme systems have shown that the intensities of the protein bands in the

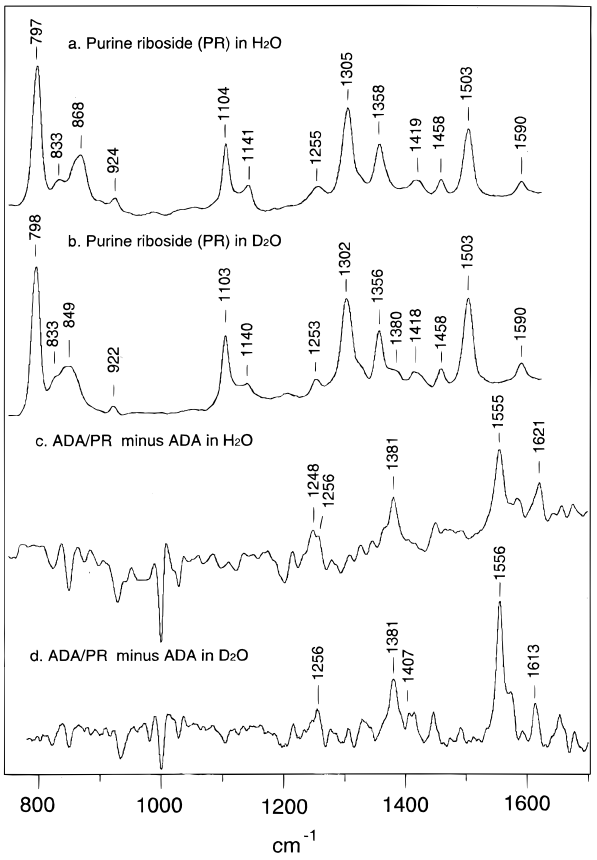

FIGURE 1: (a) Raman spectrum of PR in H_2O solution (200 mM) at 4 °C pH 7.5. (b) Same as in (a) except the sample was in D_2O. (c) Difference Raman spectrum between ADA/PR and ADA ([ADA]/[PR] = 4 mM/3.5 mM) at 4 °C in 20 mM Tris buffer, pH 7.5; and (d) same as in (c) except the sample was prepared in D_2O.

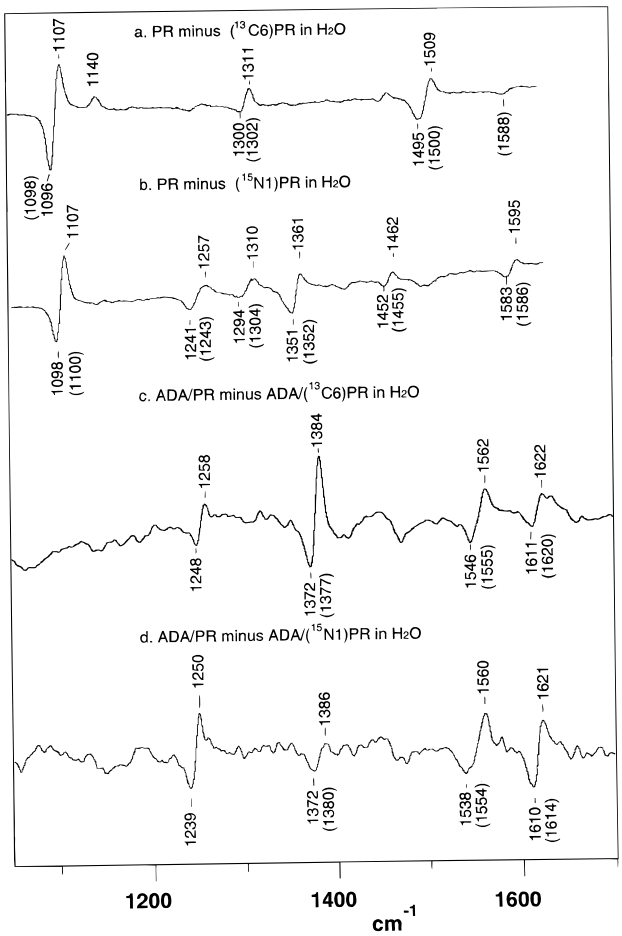

FIGURE 2: (a) Difference Raman spectrum between PR and (^{13}C6)PR in H_2O. The sample conditions are the same as in Figure 1a. (b) Difference Raman spectrum between PR and (^{15}N1)PR in H_2O. (c) Difference Raman spectrum between ADA/PR and ADA/(^{13}C6)PR in H_2O. The sample conditions are the same as in Figure 1c. (d) Difference Raman spectrum between ADA/PR and ADA/(^{15}N1)PR in H_2O. The sample conditions are the same as in Figure 1c. The frequencies in parentheses are the band positions of the isotopic labeled PRs in solution (a and b) and in the difference spectra between its ADA complex and ADA (c and d).

difference spectrum between enzyme/inhibitor complex and apoenzyme are typically on the order of 1% of the most intense protein amide-I band (this broad band, located at ca. 1620−1680 cm^{-1}, subtracts out in the difference spectra presented herein) while the intensities of the major Raman bands of purine-based nucleotides in such difference spectra are larger, on the order of 3% or more (*12*, *13*). Since the intensities of several strong bands in the difference spectrum between ADA/PR and apo-ADA, such as the bands at 1381, 1555, and 1620 cm^{-1} (Figure 1c), are more than 2% of the intensity of the protein amide-I band, they can probably be assigned to the vibrational modes of the ADA-bound PR.

To find out which of the other bands observed in the difference spectrum between the ADA/PR complex and apo-ADA (Figure 1c) are also from the bound inhibitor, isotopically labeled PR's (at N1 or C6 position) are used in the following experiments. In these experiments, two Raman spectra of ADA/PR complexes, one with the unlabeled and the other with labeled PR, are obtained. The difference spectrum between these two Raman spectra is then calculated. Such a difference spectrum only shows those bands (generally a positive/negative derivative feature) associated with the motions of the isotopically labeled atom. The difference spectra between unlabeled PR and ^{13}C6- or ^{15}N1-labeled PR spectra in H_2O solution are shown in Figure 2a or Figure 2b, respectively. Figure 2c and Figure 2d show the difference spectra between ADA/PR and ADA/(^{13}C6)-PR and between ADA/PR and ADA/(^{15}N1)PR, respectively, obtained in H_2O. The results of the same experiments performed on the samples suspended in D_2O are shown in Figure 3.

The largest derivative feature in Figure 2a is the 1107/1096 cm^{-1} pair, which indicates that the 1104 cm^{-1} band in the solution PR spectrum (Figure 1a) is sensitive to ^{13}C labeling at C6. Since this 1104 cm^{-1} band is also sensitive to ^{15}N labeling at N1 (Figure 2b), it can be assigned to the N1−C6 stretching mode. The derivative feature at 1509/1495 cm^{-1} in Figure 2a indicates that the band at 1503 cm^{-1} in Figure 1a is also sensitive to ^{13}C labeling at C6. Since the 1503 cm^{-1} band is not sensitive to the ^{15}N labeling at N1 (Figure 2b), its normal mode apparently contains C5−C6 stretch motion. Other major solution PR bands in the region above 1000 cm^{-1} in Figure 1a do not shift significantly upon ^{13}C labeling at C6 and show little features in Figure 2a. Thus, these bands have very limited contribution from the motions of C6 in the purine ring. Similarly, based on the derivative features found in the difference spectrum presented in Figure 2b arising from the ^{15}N1 label, the solution PR bands at 1255, 1358, 1458, and 1590 cm^{-1} (Figure 1a) involve motions of N1. Furthermore, it can be

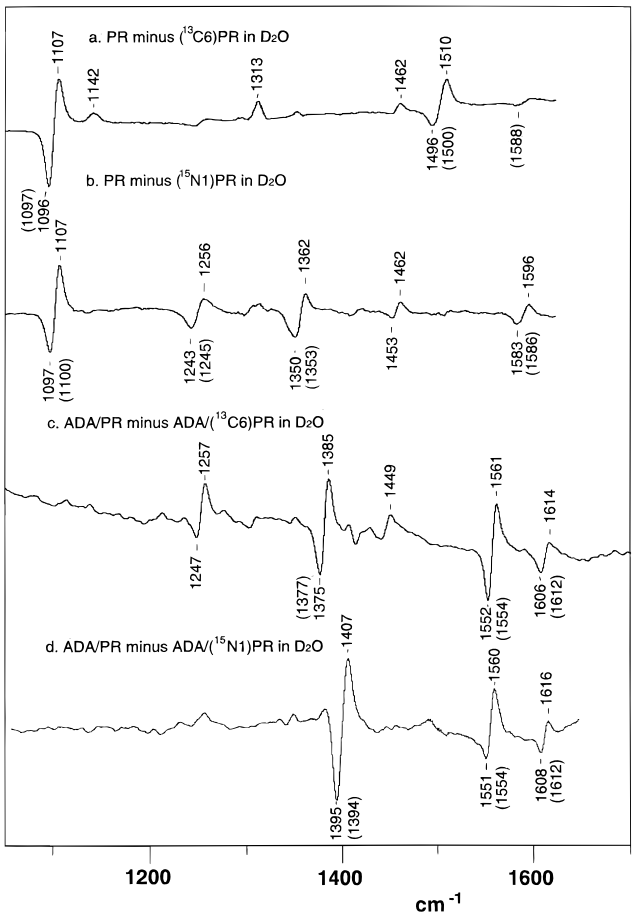

FIGURE 3: (a) Difference Raman spectrum between PR and (^{13}C6)PR in D_2O. The sample conditions are the same as in Figure 1b. (b) Difference Raman spectrum between PR and (^{15}N1)PR in D_2O. (c) Difference Raman spectrum between ADA/PR and ADA/(^{13}C6)PR in D_2O. The sample conditions are the same as in Figure 1d. (d) Difference Raman spectrum between ADA/PR and ADA/(^{15}N1)PR in D_2O. The sample conditions are the same as in Figure 1d. The frequencies in parentheses are the band positions of the isotopic labeled PRs in solution (a and b) and in the difference spectra between its ADA complex and ADA (c and d).

seen that these bands are not sensitive to the ^{13}C labeling at C6 of the purine ring (see Figure 2a); thus, they are not related to C6 motion. Since all features in Figure 2a,b are reproduced in Figure 3a,b, respectively, where the samples are suspended in D_2O, we conclude that there is no exchangeable hydrogen on N1 for PR in solution, as expected.

In the difference spectrum between the two enzyme/inhibitor complexes, with unlabeled and ^{13}C6-labeled PR, there are four derivative features at 1258/1248, 1384/1372, 1562/1546, and 1622/1611 cm^{-1}, respectively (Figure 2c). Since these derivative features must be from the vibrational modes involving the motions of the C6 atom of the PR bound in ADA, we thus confirm that the major bands at 1381, 1555, and 1621 cm^{-1} in the difference spectrum between ADA/PR and apo-ADA (Figure 1c) are indeed due to the vibrational modes from bound PR. Furthermore, this spectrum also shows that the relatively weak band at 1256 cm^{-1} in Figure 1c originates from the bound PR. There are three derivative features at 1250/1239, 1560/1538, and 1621/1610 cm^{-1} in the difference spectra between the enzyme complexes with unlabeled and ^{15}N1-labeled PR (Figure 2d). Such results indicate that the bands at 1555 and 1621 cm^{-1} in the bound PR spectrum (Figure 1c) are vibrational modes associated with both the N1 and C6 motions of the purine ring. In contrast, the 1258 and 1385 cm^{-1} bands in the bound PR spectrum (Figure 1c) are vibrational modes that have little or no contribution from N1 motion while the band at 1248 cm^{-1} in Figure 1c is due to a vibrational mode which involves N1 but not C6 motion.

When the difference spectrum between ADA/PR and ADA/(^{13}C6)PR is obtained from the samples prepared in D_2O, three of the four derivative features at 1257/1247, 1385/1375, and 1561/1552 cm^{-1} (Figure 3c) are virtually unchanged from those in Figure 2c while the derivative feature at 1614/1606 cm^{-1} is a few cm^{-1} lower than its counterpart in Figure 2c at 1622/1611 cm^{-1}. This suggests that the bound PR band at 1621 cm^{-1} (Figure 1c), which shifts down to 1613 cm^{-1} (Figure 1d) upon deuteration of the sample, is likely associated with an N−H bending motion of the bound purine ring. In other words, one of the purine nitrogens is protonated when PR is bound to ADA. This conclusion is strengthened by the difference spectrum between ADA/PR and ADA/(^{15}N1)PR complexes prepared in D_2O (Figure 3d). In this difference spectrum, a new major derivative feature at 1407/1395 cm^{-1} (Figure 3d) appears which is not observed in Figure 2d. In addition, the derivative feature at 1250/1239 cm^{-1} in Figure 2d disappears when the sample is deuterated (Figure 3d).

The differences between the Raman spectra of PR in solution (Figure 1a,b) and PR bound in ADA (Figure 1c,d) are simply too drastic to be explained by the vibrational mode shifts of the same molecule in a different environment. In a normal case, except for the frequencies related to a few highly polarizable bonds, such as C═O, C═N, N−H, and O−H bonds, most of the Raman bands of a ligand shift by less than 20 cm^{-1} upon binding to a protein, and the general spectral pattern is preserved (unless new covalent bonds are formed). In the present study, the two major solution purine bands at 1305 and 1503 cm^{-1} in Figure 1a can only find their possible counterparts more than 50 cm^{-1} away in the bound PR spectrum (see frequency-labeled bands in Figure 1c), and the other two major bands at 797 and 1104 cm^{-1} in the solution PR spectrum (Figure 1a) have completely disappeared for ADA-bound PR (Figure 1c). Furthermore, none of the Raman bands of the purine ring that are related to motions of either N1 or C6 is sensitive to the deuteration of PR in solution (compare Figure 2a,b with Figure 3a,b, respectively) while there are two deuteration-sensitive bands of ADA-bound PR, at 1256 and 1621 cm^{-1} (compare Figure 2c,d with Figure 3c,d, respectively).

On the bases of above observations, we conclude that the molecular structure of the purine ring undergoes large changes when PR binds to ADA and, moreover, one of the purine ring nitrogens protonates. One possible change of the purine ring upon PR binding to ADA is the addition of a hydroxide group to the C6 carbon to form 6-hydroxyl-1,6-dihydropurine (DHPR), as suggested by NMR and X-ray crystallographic studies (*2*, *3*). Since the aromaticity of the pyridinium ring in the purine moiety is destroyed upon the addition of the hydroxyl group on C6, large vibrational mode pattern changes are expected. However, DHPR is unstable in solution (*4*). To find out the changes that occur spectroscopically when purine is hydrated to yield DHPR, Raman measurements on a stable model compound, 6-meth-

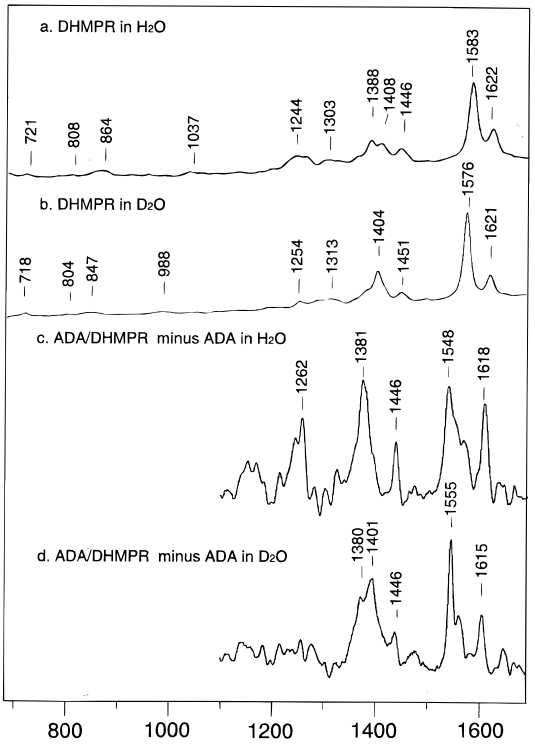

FIGURE 4: (a) Raman spectrum of DHMPR in H_2O solution (200 mM) at 4 °C, pH 7.5. (b) Same as in (a) except the sample was in D_2O. (c) Difference Raman spectrum between ADA/DHMPR and ADA ([ADA]/[DHMPR] = 4 mM/3.5 mM) at 4 °C in 20 mM Tris buffer, pH 7.5. (d) Same as in (c) except the sample was prepared in D_2O.

oxyl-1,6-dihydropurine ribonucleoside (DHMPR), were conducted both in solution and in enzyme.

Figure 4a and Figure 4b show the Raman spectra of DHMPR in H_2O and in D_2O, respectively. The band at 864 cm^{-1} in Figure 4a, which shifts down to 847 cm^{-1} upon sample deuteration (Figure 4b), can be assigned to the ribose mode which is analogous to the band at 868 cm^{-1} in the PR spectrum (Figure 1a). Since the intensities of the Raman bands of 6-methoxyl-1,6-dihydropurine are higher those of ribose, most of the major Raman bands, especially the bands at 1583 and 1622 cm^{-1}, can be assigned to the vibrational modes of the dihydropurine ring.

Figure 4c and Figure 4d show the difference Raman spectra between ADA/DHMPR and ADA in H_2O and D_2O, respectively. It is obvious that the spectrum of the ADA-bound DHMPR (Figure 4c) is very similar to that of the ADA-bound DHPR (Figure 1c). Based on such spectral similarities, it is reasonable to suggest that the ADA-bound DHPR also contains a 1,6-dihydropurine ring, and in addition, the major Raman peaks at 1262, 1381, 1446, 1548, and 1618 cm^{-1} in Figure 4c can be assigned to the vibrational modes of bound DHMPR. Upon deuteration of the enzyme complex, several changes are observed: a new Raman band appeared at 1401 cm^{-1} (Figure 4d), analogous to the band at 1404 cm^{-1} in solution (Figure 4b); the 1548 cm^{-1} band in Figure 4c shifts up by 7 cm^{-1} to 1555 cm^{-1} (Figure 4d); and the 1618 cm^{-1} band in Figure 4c shifts down by 3 cm^{-1} to 1615 cm^{-1} (Figure 4d). Comparing the spectrum of DHMPR in solution and in ADA in the double bond stretch mode region (1500−1700 cm^{-1}), it can be seen that the largest changes occur to the band at 1583 cm^{-1} (Figure 4a). This band not only shifts down by 35 cm^{-1} upon binding (Figure 4a,c) but also has an upward deuterium shift (Figure 4c,d), opposite of that observed in solution (Figure 4a,b).

Table 1 summarizes the positions of bands, and their shifts upon isotopic labeling, in the 1500−1700 cm^{-1} region for DHMPR in solution, and for DHPR or DHMPR bound to ADA. Since C═C or C═N stretches are expected in this region, the two observed modes should contain C2═N3, C4═C5 stretches or their combinations (see Scheme 1). It is well-known that the N−H bending motion of a C═N−H moiety can strongly couple with the C═N stretch because the stretch and bend frequencies are often quite close. Such coupling is substantially decreased by deuterium exchange of the hydrogen, resulting in a downshift of the N−H bend and either a downward or an upward shift of the C═N stretch mode depending if the intrinsic N−H bend frequency is below or above the C═N stretch, respectively. Mode−mode coupling generally 'pushes' apart the frequencies of the two modes. For example, deuterium exchange of protonated Schiff bases results in downshifts of the C═N stretch mode of 12−35 cm^{-1} (*14*−*16*), depending on the compound and the environment of the Schiff base. Although the exchangeable hydrogen in DHPR or DHMPR is not on the C═N bond (Scheme 1), there is apparently significant coupling between N1−H bending and the mode containing C2═N3/C4═C5 stretching motions, which is likely fairly delocalized (see below).

For DHMPR in solution, the 1622 cm^{-1} mode is essentially unaffected by deuteration of N1−H while the 1583 cm^{-1} mode shifts down by 7 cm^{-1} (Figure 4a,b). Thus, the 1583 cm^{-1} mode contains considerable N1−H bend. For DHPR in ADA, the higher frequency 1621 cm^{-1} mode shifts down by 8 cm^{-1} upon deuteration (Figure 1c,d); therefore, it is this mode which contains a substantial amount of N1−H bend. For DHMPR in ADA, the 1548 cm^{-1} band shifts up by 7 cm^{-1} while the 1618 cm^{-1} bond shifts down by 3 cm^{-1} (Figure 4c,d); thus, both of these modes contain a contribution from the N1−H bend.

On the basis of the above description of the coupling between coordinates (and calculations found below), the observed deuterium shifts of the C2═N3 and C4═C5 stretch bands in the DHPR and DHMPR spectra are interpreted as follows: in solution, the N−H bending mode is generally believed to be near 1500 cm^{-1} (see, e.g., ref *17*), although its intensity is often too low to be observed in the Raman spectrum (*18*), as is the case for DHMPR (Figure 4a). The N1−H bend is coupled with the C2═N3 stretch in DHMPR which shows up at 1583 cm^{-1} (Figure 4a), a frequency higher than its intrinsic frequency. Upon deuteration, the intrinsic N1−D bending frequency shifts down to be below 1100 cm^{-1}, and the C2═N3 stretch frequency downshifts to its intrinsic frequency at 1576 cm^{-1} (Figure 4b). In the spectrum of DHMPR bound to ADA, the two stretch bands at 1548 and 1618 cm^{-1} (Figure 4c) shift toward each other upon deuteration (Figure 4d). Thus, the frequency of the N1−H bend lies between these two stretches, i.e., somewhere between 1560 and 1610 cm^{-1}. Hence, the N1−H bending mode of DHMPR shifts up by 50 cm^{-1} to 100 cm^{-1} when bound to ADA, presumably because of the stronger hydrogen bonding of its N1−H bond for bound inhibitor compared to that found in solution. Since the Raman band frequencies and their deuterium shifts in the C═C/C═N stretch region

Table 1: Observed and Calculated Isotopic Shifts (in cm^{-1}) of the Modes of DHMPR and DHPR in the 1500−1700 cm^{-1} Region[a]

	observed			calculated			
isotope	DHMPR	DHMPR in ADA	DHPR in ADA	DHMPR	DHMPR + Cl^-	DHPR	DHPR + Cl^-
Native	1583	1548	1555	1768	1673	1740	1696
	1622	1618	1621	1776	1773	1771	1757
^{13}C6	−	−	−1	+1	−2	−2	−5
	−	−	−1	−2	−2	−1	−4
^{15}N1	−	−	−1	+1	−5	−1	−2
		−	−7	−1	−2	−2	−6
N1D	−7	+7	+1	−24	+3	−11	−4
	−1	−3	−8	−1	−5	−12	−8
^{13}C6,N1D	−	−	−1	0	−2	−1	−3
	−	−	−1	−2	−2	−2	−2
^{15}N1,N1D	−	−	−2	0	−3	0	−1
	−	−	−1	0	−1	−1	−1

[a] The observed isotopic shifts of the modes of the solution DHMPR, DHMPR, or DHPR bound in ADA are compared to those those from ab initio calculations at the HF/3-21g level for isolated DHMPR and DHPR, and complexed with Cl^- (see Scheme 1). The frequency shifts in ^{13}C6-, ^{15}N1-, and N1D-labeled compounds are relative to the native compound, while the frequency shifts in ^{13}C6,N1D- and ^{15}N1,N1D-labeled compounds are relative to the N1D-labeled compound.

are similar in the spectra of DHPR and DHMPR that are bound in ADA (Figures 1c,d and 4c,d), it is reasonable to suggest that the hydrogen bonding on the N1−H bond of DHPR is likewise strengthened when it binds to the enzyme.

Similarly, a C−H bending mode of solution DHMPR, likely the C6−H or C2−H bend, is also coupled with the N1−H bend. In this case, the intrinsic frequency of the C−H bend is close to but lower than that of the N1−H bend so that its frequency is pushed down to 1446 cm^{-1} because of the coupling (Figure 4a). Upon deuteration, the C−H bend is decoupled from the N1−D bend, and its frequency shifts back up to its intrinsic frequency at 1451 cm^{-1} (Figure 4b).

Theoretical Calculations. To better understand the changes in the Raman spectrum of DHPR when it binds to ADA and also to study the effect of the perturbations on the vibrational modes of DHPR or DHMPR in ADA, we have carried out preliminary ab initio normal-mode analyses. Our analyses are conducted on the model compounds shown in Scheme 1, with the ribose moiety replaced by a CH_2OH group to save computer time. In the analyses, the geometries of the model compounds are first optimized at the HF/3-21 g level, and the frequency calculations are then performed on the optimized geometries using the same basis set. It is well-known that such calculations consistently overestimate stretching force constants by about 20% and the frequencies by about 10%. Normally, this can be corrected for by 'scaling' the force constants to fit the experimental data (cf. *19*). However, the Raman data on 6-hydroxyl-1,6-dihydropurine ribonucleoside in solution are not available because this compound is not stable, and the Raman data on the ADA-bound DHPR are incomplete, limited only to a few bands related to N1 and/or C6 motion. The Raman data on DHMPR are also limited. Thus, there are not enough constraints to perform the scaling of the force field to obtain correct normal modes. Nevertheless, the assignments of the Raman bands observed in the experiments can often be achieved by ab initio normal-mode calculations based on the comparisons between the relative frequency orders, the relative Raman band intensities, and especially the isotopic shifts of the observed and calculated frequencies (*17*, *20*).

The results of the calculations for DHPR, DHMPR, and their complexes with Cl^- ion (Scheme 1) suggest that the two most intense bands in the 1500−1700 cm^{-1} region (after multiplying the calculated frequencies by a factor of 0.9, see above) are the C2═N3 and the C4═C5 stretches. Their frequencies and the isotopic shifts are shown in Table 1. The calculations on the DHPR(DHMPR)/Cl^- complex are an attempt to mimic the hydrogen bonding environment of N1 in ADA; the Cl^- ion is fixed to the position of Oδ1 of Glu217 relative to the N1 nitrogen of the ADA-bound DHPR, as determined by X-ray crystallographic studies (*3*).

The calculations show that for DHPR, there are two vibrational modes in the 1500−1700 cm^{-1} region that have significant Raman intensities. The higher frequency mode at 1771 cm^{-1} is the C2═N3 stretch mode which also contains a contribution from the N1−H bend. The lower frequency mode at 1740 cm^{-1} is the C4═C5 stretch mode which also contains a contribution from the N1−H bend. The calculated low-intensity N1−H bending mode is at 1663 cm^{-1}, lower than both the C2═N3 and the C4═C5 stretch modes. Hence, deuteration of N1−H leads to a significant downshift in both stretch modes. The same calculation on isolated DHMPR yielded similar but somewhat different results. In this case, the higher frequency mode at 1776 cm^{-1} is the C4═C5 stretch which contains no contribution from the N1−H bend while the lower frequency mode at 1768 cm^{-1} is the C2═N3 stretch which has significant contribution from the N1−H bend. The calculated N1−H bend is at 1655 cm^{-1}. Thus, only the lower frequency mode has significant downshift upon deuterium labeling, in agreement with the Raman results from DHMPR in solution (Table 1).

For DHPR complexed with Cl^-, The higher frequency mode at 1757 cm^{-1} is the C4═C5 stretch, coupled with the N1−H bend, resulting in a 8 cm^{-1} shift upon deuteration, in good agreement with the experimental results (Table 1). The lower frequency mode at 1696 cm^{-1} becomes the in-phase combination of the C4═C5 and C2═N3 stretches with little contribution from the N1−H bend. The N1−H bend in the Cl^- complex shifts up to 1748 cm^{-1}, but with quite significant contribution from the out-of-phase combination of the C2═N3 and the C4═C5 stretches. However, the calculations do not correctly predict the deuterium shift of the lower frequency mode (−4 cm^{-1}) for the ADA-bound DHPR (+1 cm^{-1}; Table 1).

For the DHMPR/Cl^- complex, the calculated higher frequency C4═C5 stretch mode shifts down by 3 cm^{-1} compared to the isolated form and becomes coupled with the N1−H bend. Upon deuteration, this mode shifts down by 5 cm^{-1}, in very good agreement with experiments (Table 1). The calculated lower frequency C2═N3 stretch mode shifts down by 95 cm^{-1} to 1673 cm^{-1} in the presence of the Cl^- ion and has only a small contribution from the N1−H bend. The calculated N1−H bending mode shifts up to 1736 cm^{-1} in the Cl^- complex, higher than the C2═N3 stretch but lower than the C4═C5 stretch. Upon deuteration, the lower frequency C2═N3 stretch shifts up by 3 cm^{-1}, and the higher frequency C4═C5 stretch shifts down by 5 cm^{-1}. This is in reasonably good agreement with the results observed in the ADA-bound DHMPR (Table 1) and consistent with the description of the coupling between N1−H and C═N/C═C stretch modes discussed in detail in the previous section. The smaller upward shift of the lower frequency mode compared to that observed in the spectra of ADA-bound DHMPR (Table 1) is likely due to the fact that the Cl^- ion is too close to the N1−H bond in the model complex so that the N1−H bending mode frequency becomes too high and its coupling with the lower frequency mode is thus underestimated. In fact, when the Cl^- ion is moved away from the N1−H bond in the model complex, the calculated upward shift of the lower frequency mode does increase, for example, to 5 cm^{-1} when the Cl^- ion is 3.17 Å away from N1. Thus, the results of the calculations support our interpretations on the observed deuterium shifts of the C2═N3 and C4═C5 stretch bands in the spectra of DHPR or DHMPR bound to ADA.

Similar calculations using the larger 6−31 g** basis set produced less satisfactory results. The main reason is that calculated C═N stretching frequencies by this basis set are much higher relative to the N−H bending frequencies. As a result, the C2═N3 stretch mode can never shift down to a frequency lower than the N1−H bending frequency. Hence, the deuterium shift of the C2═N3 stretch is always toward the lower frequency regardless of the placement of the Cl^- ion in the model complex.

DISCUSSION

Our results show that the N1−H bending frequency of the ADA-bound DHMPR and DHPR shifts up by 50−100 cm^{-1} compared to its frequency in aqueous solution. Such a frequency shift is the result of stronger hydrogen bonding to the N1−H bond of the inhibitor in the enzyme compared to that found in solution. Since ADA/DHPR is considered as a transition state analogue, this strengthened hydrogen bonding may contribute to the stabilization of the transition state. Thus, it would be interesting to determine the hydrogen bonding strength in the enzyme quantitatively.

There have been several studies quantitatively correlating the shifts of the N−H (or O−H) stretch frequency to the enthalpic energy of hydrogen bond formation (cf. *5*, *21*, *22*). It has been determined that every 100 cm^{-1} shift in the stretching frequency corresponds to 1.1−1.3 kcal/mol in energy, depending on the exact molecular system. It has also been noticed in earlier experiments that stronger hydrogen bonding to the O−H or N−H bond causes an increase in its bending mode frequencies (cf. *23*−*26*). Although a direct quantitative relationship between the hydrogen bonding enthalpies and the O−H or N−H bending frequencies has not been firmly established, it is still possible to estimate the hydrogen bonding energy change on the basis of the O−H or N−H bending frequency change though indirect methods, using the relationship between stretching frequency and hydrogen bonding energy and the relationship between stretching and bending frequencies. The correlation between stretching and bending frequency shifts can be estimated by observation of the water molecule. Water dissolved in carbon tetrachloride has two stretching modes at 3755 and 3650 cm^{-1} and a bending mode at 1595 cm^{-1} (*22*). In an aqueous environment, the H−O−H stretching bands are centered around 3425 and 3275 cm^{-1}, a downward shift of about 360 cm^{-1}, while the H−O−H bending mode shifts upward by 50 cm^{-1} to 1645 cm^{-1}. Thus, every cm^{-1} upward shift of the bending mode frequency corresponds roughly to a 7.2 cm^{-1} downward shift of the stretching mode frequency. By combining the two correlations, we obtain an approximate correlation between the bending frequency shift and interaction energy change: every 10 cm^{-1} shift of the bending frequency corresponds to about 0.8−1.0 kcal/mol change of the energy. Therefore, the 50−100 cm^{-1} upward shift of the N1−H bending frequency of the bound DHMPR or DHPR corresponds, approximately, to 4−10 kcal/mol of hydrogen bonding energy in the N1−H bond upon forming the enzyme complex over that in aqueous solution.

In the proposed reaction mechanism of ADA-catalyzed deamination of adenosine (*3*, *27*), the COOH group of Glu217 interacts with N1 of adenosine in the ground state upon binding of adenosine; the COOH group subsequently donates the proton to N1 followed by the attack of a hydroxide to the C6 of adenosine to form the transition state (or reaction intermediate). (Simultaneous proton and hydroxide additions are also possible.) Since the purine ring is protonated at N1 and its C6 carbon is tetrahedral in the ADA/DHPR complex, it is believed to be an analogue to the transition state (or the intermediate). Assuming that the interaction energy between the COOH group of Glu217 and the N1 of adenosine in the ground state of the ADA/adenosine complex is similar to the interaction between N1−H of DHPR and a water molecule in solution, and if the interaction between N1−H of DHPR and COO^- of Glu217 in the ADA/DHPR complex is comparable to that between adenosine and enzyme in the transition state, our Raman results then suggest that the interaction between COO^- of Glu217 and N1−H of hydrated adenosine can reduce the transition state energy by up to 4−10 kcal/mol if entropic effects are ignored.

This estimation of the transition state stabilization contribution of the interaction between Glu217 of ADA and N1−H of substrate is in reasonable agreement with previous studies on a number of Glu217 mutants of mouse ADA (*6*). These studies have shown that when Glu217 is mutated to either Asp, Ala, or Arg, the value of K_m changes only slightly but k_{cat} is decreased substantially. It has been clearly established that the rate-limiting step in determining k_{cat} is the enzymic chemistry along the reaction pathway as opposed to product release (*7*, *28*). In view of the similarities of sequence and active site residues between the calf enzyme and mouse enzyme studied herein, it seems unlikely there is

any difference in mechanism between the two enzymes. Hence, it is reasonable to compare the present results with previous studies on the calf enzyme and to ascribe results on mutant enzymes on k_{cat} as resulting from changes of the transition state barrier height. For example, in the Glu217Asp mutant, k_{cat} is reduced by 700-fold. The 700-fold reduction of k_{cat} corresponds to a 3.9 kcal/mol destabilization of the transition state, just under the value estimated from our current Raman studies.

In addition, inverse solvent (D_2O) isotope effects are observed (*7*, *28*−*30*) for both k_{cat} and the K_d's of inhibitor binding (calf enzyme). The source of these isotope effects has been the subject of considerable speculation (*29*−*31*). The fractionation factors for several different exchangeable hydrogens need assignment to fully explain the data. For the enzymatic ground state, the needed fractionation factors are those for the active site zinc-bound water and protonated Glu/Asp217. For the transition state complex or complexes with the transition state analogue, the fractionation factors needed are those for the hydrogen bond between the Zn and the hydrated inhibitor transition state, and for the hydrogen bond between Glu217 and the N1−H bond of the inhibitor. If the Glu217 hydrogen bond is within range of a normal hydrogen bond with a harmonic potential, the greater strength observed in the complex with the transition state analogue which we have deduced from the Raman experiments would indeed contribute to tighter binding in D_2O in accord with observation. The heteroatom distances in this hydrogen bond (*3*) are not unusually short, and the band positions and deuteration shifts observed in the Raman results herein are high but within a 'normal' range, suggesting that it has a normal parabolic potential. Therefore, it is likely that the increased strength deduced from the Raman experiments does contribute to the observed inverse solvent isotope effects. However, a complication arises from the possibility that the hydrogen bond at the zinc-hydrated inhibitor is a low-barrier hydrogen bond with an abnormally low fractionation factor arising from the marked anharmonic potentials expected of such bonds (*31*, *32*). The Zn−O distance of this bond in the complex is very short, and the presence of such a bond in the transition state or its analogue complex might give rise to a normal (greater than 1) solvent isotope effect. Future Raman experiments may address this issue.

APPENDIX

We show in this section the procedure used to obtain the difference spectra presented in the main article. In general, Raman difference spectroscopy requires a high degree of precision in calculating the difference spectrum, and it is necessary that the instrument be calibrated to ensure that neither systematic noise factors nor shot noise are mistaken for small difference peaks. Our Raman difference spectrometer has been shown to produce difference spectra having noise-to-signal ratios as small as 0.1% of the protein amide-I peak (*5*). We show here the control procedures that were performed in determining the data of Figure 1c. All the other difference spectra presented herein underwent the same procedures.

In each difference Raman experiment, the ADA/PR complex and ADA (or ADA/labeled PR) were loaded into a split Raman cell, and the Raman spectra were taken alternatively from the two samples (*5*). Up to 10 runs were taken from each sample, and they were then summed and averaged. The averaged spectrum so obtained for the ADA/PR complex is shown in Figure 5a while Figure 5b shows that of ADA. As a control experiment, the odd-numbered runs and even-numbered runs on the ADA/PR sample were averaged, and their difference spectrum is shown in Figure 5c (enhanced by a factor of 20). This difference spectrum should null completely; in fact, the noise in this spectrum, all of which is simple shot noise and is free from systematic subtraction artifacts, is 0.2% of the amide-I band of ADA, which is more than adequate for the present studies.

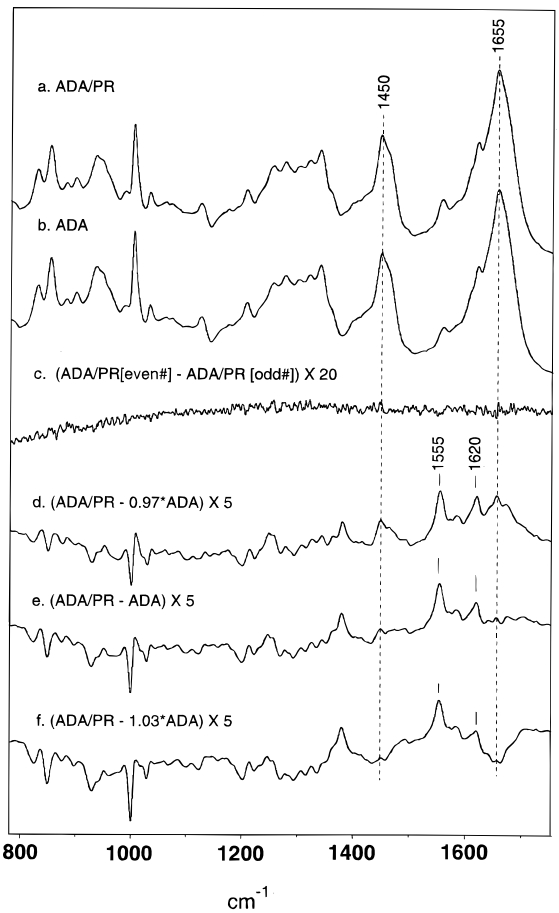

FIGURE 5: (a) Raman spectrum of ADA/PR. (b) Raman spectrum of ADA. (c) Difference spectrum of even-numbered ADA/PR runs minus odd-numbered runs; the results were then multiplied by a factor of 20. (d) Difference spectrum between ADA/PR and ADA; a factor of 0.97 was multiplied on the ADA spectrum, and the result was multiplied by a factor of 5. (e) Difference Raman spectrum between ADA/PR and ADA, same as Figure 1c. (f) Difference spectrum between ADA/PR and ADA; a factor of 1.03 was multiplied on the ADA spectrum, and the result was multiplied by a factor of 5.

In the subtraction process, two Raman bands were used as internal references, the amide-I band at 1655 cm^{-1} and the δCH band at 1450 cm^{-1}. A multiplication factor was applied to one of the spectra and adjusted so that in the final difference spectrum these two bands were no longer visible. Since the peak to peak intensity in the spectrum of the control (Figure 5c) is about 0.2% of the 1655 cm^{-1} band intensity of the original spectrum, we expect the noise level in the ADA/PR minus ADA difference spectrum to be the same. Figure 5e shows the ADA/PR minus ADA difference spectrum, with both 1450 and 1655 cm^{-1} bands subtracted

properly. Figure 5d,f shows the slightly under-subtracted and over-subtracted difference spectra, respectively. In these two spectra, both 1450 and 1655 cm^{-1} bands are clearly visible, either positive or negative. The intensities of the spectra in Figure 5d−f were enhanced by a factor of 5 relative to the scale of Figure 5a for clarity. The intensities of the 1555 and 1620 cm^{-1} bands in Figure 5e are 5.5% and 2.5%, respectively, of the intensity of the original spectrum's amide-I peak centered at 1655 cm^{-1}. Since the noise level in these difference spectra should be on the order of 0.2% of the 1655 cm^{-1} band intensity based on the estimation in our control experiment, we concluded that in Figure 5e, the peaks with an intensity larger than 0.2% of the 1655 cm^{-1} band intensity of the original spectrum are real Raman bands either from bound PR or from ADA which has been perturbed by binding the PR inhibitor.

REFERENCES

1. Frieden, C., Kurz, L. C., and Gilbert, H. R. (1980) *Biochemistry 19*, 5303.
2. Kurz, L. C., and Frieden, C. (1987) *Biochemistry 26*, 8450−8457.
3. Wilson, D. K., Rudolph, F. B., and Quiocho, F. A. (1991) *Science 252*, 1278−1284.
4. Jones, W., Kurz, L. C., and Wolfenden, R. (1989) *Biochemistry 28*, 1242−1247.
5. Callender, R., and Deng, H. (1994) *Annu. Rev. Biophys. Biomol. Struct. 23*, 215−245.
6. Mohamedali, K. A., Kurz, L. C., and Rudolph, F. B. (1996) *Biochemistry 35*, 1672−1680.
7. Kurz, L. C., Weitkamp, E., and Frieden, C. (1987) *Biochemistry 26*, 3027−3032.
8. Gordy, W. (1946) *J. Chem. Phys. 14*, 305−320.
9. Roy, S., Papastavros, M. Z., Sanchez, V., and Redfield, A. G. (1984) *Biochemistry 23*, 4395−4400.
10. Yue, K. T., Deng, H., and Callender, R. (1989) *J. Raman Spectrosc. 20*, 541−546.
11. Frisch, M. J., Trucks, G. W., Head-Gordon, M., Gill, P. M. W., Wong, M. W., Foresman, J. B., Johnson, B. G., Schlegel, H. B., Robb, M. A., Replogle, E. S., Gomperts, R., Andres, J. L., Raghavachari, K., Binkley, J. S., Gonzalez, C., Martin, R. L., Fox, D. J., Defrees, D. J., Baker, J., Stewart, J. J. P., and Pople, J. A. (1994) *Gaussian 94, Revision D*, Gaussian, Inc., Pittsburgh, PA.
12. Yue, K. T., Yang, J. P., Charlotte, M., Lee, S. K., Sloan, D., and Callender, R. (1984) *Biochemistry 23*, 6480−6483.
13. Deng, H., Zheng, J., Burgner, J., Sloan, D., and Callender, R. (1989) *Biochemistry 28*, 1525−1533.
14. Aton, B., Doukas, A., Narva, D., Callender, R., Dinur, U., and Honig, B. (1980) *Biophys. J. 29*, 79−94.
15. Benecky, M. J., Copeland, R. A., Hays, T. R., Lobenstine, E. W., Rava, R. P., Pascal, R. A. J., and Spiro, T. G. (1985) *J. Biol. Chem. 260*, 11663−11670.
16. Baasov, T., Friedman, N., and Sheves, N. (1987) *Biochemistry 26*, 3210−3217.
17. Deng, H., Huang, L., Groesbeek, M., Lugtenburg, J., and Callender, R. H. (1994) *J. Am. Chem. Soc. 98*, 4776−4779.
18. Colthup, N. B., Daly, L. H., and Wiberley, S. E. (1990) *Introduction to Infrared and Raman Spectroscopy*, 3rd ed., Academic Press, San Diego.
19. Pulay, P., Fogarasi, G., Pongor, G., Boggs, J. E., and Vargha, A. (1983) *J. Am. Chem. Soc. 105*, 7037.
20. Deng, H., Chan, A. Y., Bagdassarian, C. K., Estupinan, B., Ganem, B., Callender, R. H., and Schramm, V. L. (1996) *Biochemistry 35*, 6037−6047.
21. Joesten, M., and Schaad, L. J. (1974) *Hydrogen Bonding*, Marcel Dekker, Inc., New York.
22. Vinogradov, S. N., and Linnel, R. H. (1971) *Hydrogen Bonding*, Van Nostrand Reinhold Co., New York.
23. Pullin, J. A., and Werner, R. L. (1965) *Spectrochim. Acta 21*, 1257−1261.
24. Nozari, M. S., and Drago, R. S. (1970) *J. Am. Chem. Soc. 92*, 7086−7092.
25. Drago, R. S., and Epley, T. D. (1969) *J. Am. Chem. Soc. 91*, 2883−2887.
26. Novak, A. (1974) *Struct. Bonding 18*, 177.
27. Wilson, D. K., and Quiocho, F. A. (1993) *Biochemistry 32*, 1689−1694.
28. Weiss, P. M., Cook, P. F., Hermes, J. D., and Cleland, W. W. (1987) *Biochemistry 26*, 7378−7384.
29. Kurz, L. C., and Frieden, C. (1983) *Biochemistry 22*, 382−389.
30. Kurz, L. C., Moix, L., Riley, M. C., and Frieden, C. (1992) *Biochemistry 31*, 39−48.
31. Cleland, W. W. (1992) *Biochemistry 31*, 317−319.
32. Burgner, J. W., II, and Ray, W. J. (1974) *Biochemistry 13*, 4229−4237.

BI9727904